Macrophages expressing chimeric cytokine receptors have an inflammatory phenotype and anti-tumoral activity upon IL-10 or TGFβ stimulation

Sabrina Traxel[1], Florian Schmidt[1], Corina Beerli[1], Dinh-Van Vuong[1], Roberto F. Speck[1*], Simon Bredl [1*]

[1] Department of Infectious Diseases and Hospital Epidemiology, University Hospital Zurich, University of Zurich, Raemistrasse 100, 8091 Zurich, Switzerland

*co-senior authors

CORRESPONDING ADDRESSES:

Dr. rer. nat. Simon Bredl

Department of Infectious Diseases and Hospital Epidemiology, University Hospital Zurich, University of Zurich, Raemistrasse 100, 8091 Zurich, Switzerland

e-mail: simon.bredl@gmail.com

tel: +41 43 253 32 78

Dr. sc. nat. Sabrina Traxel

Department of Infectious Diseases and Hospital Epidemiology, University Hospital Zurich, University of Zurich, Raemistrasse 100, 8091 Zurich, Switzerland

e-mail: sabrinatraxel@gmail.com

tel: +41 43 253 44 15

DECLARATIONS

Ethics approval and consent to participate

Written consent for the use of buffy coats for research purposes was obtained from blood donors by the Blood Donation Centre.

Consent for publication

Not applicable.

Competing interests

SB and RS hold a patent associated to the ChCR (WO2024133517). No potential competing interests were declared by the other authors.

Funding

This project was funded by Gilead Swiss Fellowship (ST), UZH Postdoc grant (CB), Innosuisse 103.487 IP-LS (SB, RS), Claudia von Schilling Stiftung (SB, RS), Lotte und Adolf Hotz-Sprenger Stiftung (SB, RS), OPO Stiftung (SB, RS), Gebauer Stiftung (SB, RS), Novartis Foundation for Medical Biological Research (#19B139) (SB, RS), USZ Foundation (SB, RS), UZH Entrepreneur Fellowship (SB), Arnold U. und Susanne Huggenberger-Bischoff Stiftung (SB, RS), Peter Bockhoff Stiftung (SB, RS), Mach-Gaensslen Stiftung (SB, RS).

Authors' contributions

Conceptualization: ST, RS, SB

Chimeric cytokine receptor conceptualization and design: SB

Experiments: ST, FS, CB, VDV

Study supervision: RS, SB

Manuscript writing: ST, RS, SB

Funding acquisition: ST, CB, RS, SB

Acknowledgments

We thank the anonymous donors for donating the buffy coats. Flow cytometry was performed with equipment of the Flow Cytometry Facility, University of Zurich. We thank for the assistance in cell sorting experiments by the Flow Cytometry Facility, University of Zurich. We thank the Functional Genomics Center Zurich (FGCZ) of University of Zurich and ETH Zurich, and in particular Timothy Sykes, Hubert Rehrauer, and Peter Leary, for the support on RNA sequencing analysis. We thank Jeremy Luban for providing us with pcDNA3.1 Vpx and p8.9NDSB-DPAVDLL plasmids for virus production and Patrick Salmon for providing us with pCWX Dest backbone. We thank Patrick Turko for his advice on analysis of TCGA data. We thank Sarah Brünigk for her advice with the RNAseq data analysis. The results shown here are in part based upon data generated by the TCGA Research Network: https://www.cancer.gov/tcga. ChatGPT was used to improve wording, grammar and spelling of this manuscript.

ABSTRACT

Background

Triple-negative breast cancer (TNBC) is a highly aggressive subtype of breast cancer that lacks hormone receptors and HER2 amplification, making it unresponsive to standard hormone or HER2-targeted therapies. Although immune checkpoint inhibitors (ICIs) have shown promise in tumors with high lymphocyte infiltration, their efficacy remains limited in tumors with minimal lymphocyte infiltration. To overcome this challenge, we developed a novel approach to reprogram tumor-associated macrophages (TAMs) from an immunosuppressive to an inflammatory phenotype within the tumor microenvironment (TME), aiming to enhance therapeutic outcomes in TNBC.

Methods

We designed a chimeric cytokine receptor (ChCR) that triggers STAT1 signaling upon stimulation with IL-10 or TGFβ, cytokines prevalent in the TME that typically drive immunosuppression. Human primary macrophages were transduced with a lentiviral vector expressing the ChCR, and changes in their phenotype, secretome, and transcriptome were analyzed following stimulation. The anti-tumoral activity of these reprogrammed macrophages was assessed using co-culture assays with 3D TNBC spheroids.

Results

ChCR expressing macrophages showed robust STAT1 activation in response to IL-10 or TGFβ stimulation, resulting in an inflammatory phenotype similar to IFNγ activation, as confirmed by phenotypic markers, and transcriptomic profiling. These ChCR-stimulated macrophages demonstrated significant anti-tumoral effects in 3D TNBC spheroids. Moreover, ChCR stimulation led to the upregulation of genes associated with good response to ICIs, among others *CXCL9* and *CXCL10*, chemokines essential for lymphocyte recruitment. Secretion of CXCL10 was also confirmed by ELISA.

Conclusion

We successfully engineered a ChCR that reprograms TAMs within an IL-10- and TGFβ-rich environment, inducing an inflammatory phenotype and anti-tumoral activity. The expression of *CXCL9* and *CXCL10* further supports lymphocyte recruitment, potentially facilitating greater lymphocyte infiltration and disrupting the immunosuppressive TME. This approach offers a promising strategy to improve immunotherapy outcomes in TNBC patients, particularly those with low immune cell infiltration, thereby addressing a critical unmet clinical need.

88 **LIST OF ABBREVIATIONS**

89

90	CAR	Chimeric antigen receptor
91	ChCR	Chimeric cytokine receptor
92	EF1a	Elongation factor 1 alpha core promoter
93	FDR	False discovery rate
94	GO:BP	Gene Ontology biological process
95	hPGK	Human phosphoglycerate kinase promoter
96	ICI	Immune checkpoint inhibitor
97	MFI	Median fluorescence intensity
98	NES	Normalized enrichment score
99	NR	No response
100	PCA	Principle component analysis
101	R	Response
102	RLU	Relative light units
103	RNAseq	RNA sequencing
104	SEAP	Secreted embryonic alkaline phosphatase
105	SFFV	Spleen focus-forming virus promoter
106	TAM	Tumor associated macrophage
107	TCGA	The Cancer Genome Atlas
108	TME	Tumor microenvironment
109	TNBC	Triple negative breast cancer
110	tNGFR	Truncated nerve growth factor receptor

111 **INTRODUCTION**

112 Triple negative breast cancer (TNBC) is an aggressive subtype of breast cancer that lacks both hormone receptor expression
113 and HER2 amplification and is therefore not amenable to hormone or HER2 targeted therapies (reviewed in[1]). Current first
114 line treatment for both high-risk early-stage TNBC and advanced stage, PD-L1 positive TNBC (combined positive score
115 ≥10) is the immune checkpoint inhibitor (ICI) pembrolizumab in combination with chemotherapy. Early stage TNBC have
116 a good prognosis with 86.6% overall survival at 60 months when treated with neoadjuvant pembrolizumab and
117 chemotherapy.[2] In patients with advanced stage TNBC the pembrolizumab and chemotherapy combination improves the
118 median overall survival from 16.1 months to 23 months, when compared to the placebo and chemotherapy cohort, which
119 is still a dismal prognosis for the patients.[3] Thus, there is clearly an unmet need for patients with advanced TNBC.

120 Adoptive cell therapy using chimeric antigen receptor (CAR) T cells has achieved remarkable success in hematological
121 malignancies[4] and there was great hope that CAR T cell therapy would also change the therapeutic landscape for solid
122 tumors. To date, CAR T cells had only limited success in solid tumors.[5 6] Several phase I clinical trials of CAR-based
123 immunotherapies for TNBC are currently underway.[7] While we eagerly await the first results of adoptive CAR T cell
124 therapies in TBNC, alternative innovative treatments must be sought.

125 A critical determinant of disease progression of solid tumors including TNBCs, is their immunophenotype, which is based
126 on the number and localization of CD8+ T cells in the tumor microenvironment (TME).[8-10] Three main immunophenotypes
127 have been defined: hot (high number of intratumoral T cells), excluded (T cells restricted to the tumor margin) or cold
128 (lack of T cells).[11] Patients with a hot TME, including patients suffering from TNBC, have a better prognosis and show
129 better response to ICI treatment than patients with an excluded or cold TEM. [8 10 12-14] In TNBC, 42-54% of patients have a
130 tumor with excluded or cold immunophenotype.[8 10 15] Therefore, reprogramming a cold into a hot TME is of great
131 therapeutic interest.

132 Myeloid cells including tumor associated macrophages (TAMs) constitute up to 30% of the tumor mass.[16] TAMs
133 differentiate from monocytes that are actively recruited into the TME.[17] In general, macrophages can adopt a wide range
134 of phenotypes depending on the stimuli received and tissue environment.[18] Consequently, their activities include
135 immunosuppression, tissue repair, phagocytosis, inflammation, and cytotoxicity. Inflammatory macrophages are induced
136 by pro-inflammatory signals like IFNγ and/or LPS, whereas immunosuppressive macrophages are induced by
137 immunosuppressive cytokines like IL-4, IL-13, IL-10, or TGFβ. IL-10 and TGFβ are expressed in the TME of solid tumors,
138 such as in TNBC[19-21] and consequently push TAMs to adopt an immunosuppressive phenotype. TAMs inhibit the immune
139 system, support tumor growth, angiogenesis, and tumor cell migration (reviewed in[22]). In contrast, inflammatory
140 macrophages have anti-tumoral activity by attracting T cells, by increased antigen presentation and their direct tumoricidal
141 effects.[20 23-26] In fact, tumors with high number of inflammatory macrophages are more likely to have a hot TME, a better
142 prognosis and better response to ICIs.[8 27-29] Thus, reprogramming TAMs towards an inflammatory phenotype is a hot topic
143 in the field of cancer immunotherapy.[30]

144 We believe that macrophages should be reprogrammed to switch to inflammatory and anti-tumoral macrophages locally in
145 the TME. Systemically activated macrophages may be retained in various tissues, unable to reach their destination.
146 Furthermore, local activation would be less likely to have off-target effects. Therefore, we developed chimeric cytokine
147 receptor (ChCR) expressing macrophages that utilize immunosuppressive cytokines enriched in the TME to switch to

148 inflammatory macrophages. Specifically, we engineered macrophages to express a ChCR that binds either IL-10 or TGFβ
149 and induces an IFNγ signaling.

150

151 # MATERIALS AND METHODS

152 **Ethics statement**

153 Monocytes used were obtained from buffy coats, anonymously provided by the Blood Donation Service Zurich, Swiss Red
154 Cross, Schlieren. Written consent for the use of buffy coats for research purposes was obtained from blood donors by the
155 Blood Donation Centre.

156 **Cell lines**

157 HEK293T (ATCC) were maintained in Dulbecco′s Modified Eagle′s Medium - high glucose (DMEM, Sigma-Aldrich,
158 D6429) supplemented with 10% heat-inactivated fetal bovine serum (FBS, Gibco, 10270-106) (hereafter called D10).
159 HEK-Blue™ IFN-γ cells (Invivogen, hkb-infg)) were maintained in D10 supplemented with 100µg/ml Zeocin (Invivogen,
160 ant-zn-1) and 30µg/ml Blasticidin (Invivogen, ant-bl-1). MDA-MB-231 (ATCC) were maintained in RPMI-1640 (Sigma-
161 Aldrich, R8758) supplemented with 10% heat-inactivated FBS (Gibco, 10270-106) (hereafter called R10). BT-549
162 (ATCC) were maintained in R10 supplemented with 10ug/ml insulin (Sigma- Aldrich, I9278). THP-1 (ATCC) were
163 maintained in R10 supplemented with 2-mercaptoethanol (Gibco, 31350010). MRC-5 (ATCC-CCL-171) were maintained
164 in Eagle's Minimum Essential Medium (EMEM, ATCC-30-2003) supplemented with 10% heat inactivated FBS. All cells
165 were maintained at 5% CO_2 and 37°C in a humidified incubator.

166 **Monocyte derived macrophages**

167 Peripheral mononuclear cells were isolated from buffy coats of healthy donors (Blood Donation Service Zurich, Swiss Red
168 Cross, Schlieren) using density gradient centrifugation on lymphoprep (Axon Lab, 1858). Monocytes were isolated using
169 CD14 microbeads (Miltenyi Biotec, 130-050-201) and plated at 150’000 cells/cm^2 in F+ high attachment plates (Sarstedt)
170 in RPMI-1640 supplemented with Penicillin-Streptomycin (P/S, Gibco, 15140-122). Two hours after plating, medium was
171 replaced with RPMI-1640 supplemented with P/S and 10% human AB serum (Sigma Aldrich, H6914), hereafter called
172 RH10. Monocytes were differentiated for 6-11 days with medium change every 2-3 days. To polarize macrophages, they
173 were stimulated for additional 48h with IFNγ (Biolegend, 570204), IL-10 (Biolegend, 571004) or TGFβ1 (Peprotech, 100-
174 21) at indicated concentrations.

175 **Plasmid construction**

176 To generate ChCR plasmids, amino acid sequences of the human IL10RA, IL10RB, TGFβR1, TGFβR2, IFNGR1 and
177 IFNGR2 receptor were obtained from UniProt. Supplementary Table 1 shows Uniprot sequences used for the ChCR design.
178 The ChCR were constructed as follows: The extracellular domains of IL10RA, IL10RB, TGFβR1, or TGFβR2 were fused
179 to the transmembrane and extracellular domain of the IFNGR1 or IFNGR2, including a glycine-serine linker for
180 flexibility.[31 32] As an N-terminal signal peptide, we used the one from the corresponding intracellular IFNGR. All variants
181 were analyzed with DeepTMHMM to verify *in silico* signal peptide cleavage, transmembrane domains and surface
182 expression.[33] Sequences were ordered codon-optimized at GenScript Biotech Corporation. For expression of single chains,
183 ChCR sequences were subcloned into a pCWX Dest lentiviral vector (Gift from Patrick Salmon) under the control of an
184 elongation factor 1 alpha core promoter (EF1a). To simultaneously express both chains, ChCR sequences were subcloned
185 into a pCWX Dest lentiviral vector separated by a P2A sequence and under the control of a spleen focus-forming virus
186 (SFFV) promoter. All lentiviral vectors also encode for a truncated nerve growth factor receptor (tNGFR) driven by a

187 human phosphoglycerate kinase (hPGK) promoter as a reporter for transduction. Mock lentiviral vector only encodes for
188 tNGFR.

189 To generate the Luciferase-EGFP plasmid, luciferase and EGFP sequences, separated by a T2A sequence, were ordered as
190 gene blocks and subcloned into a pCWX Dest lentiviral vector under the control of EF1a promoter.

191 **Lentivirus production and titration**

192 Lentiviral vectors were produced in HEK293T. Briefly, 13 Million cells were plated in T150 flasks. The day after, cells
193 were co-transfected using PEI (Polysciences, 23966) with pMD2.G, p8.9NDSB-DPAVDLL[34] (gift from Jeremy Luban),
194 pcDNA3.1 Vpx239[34] (gift from Jeremy Luban) and pCWX Dest transfer vector at a molar ratio of 251:107.5:756.1:45. 4h
195 after transfection, medium was changed and supplemented with 5mM sodium butyrate (Sigma Aldrich, B5887). Virus was
196 harvested 52h after transfection and clarified by centrifugation. Lentiviral supernatants were concentrated by ultrafiltration
197 using 100kDa cut-off Amicon filters (Merck Milipore, UFC910024). Titration of lentiviruses was done by transducing
198 HEK293T. Three days after transduction, transduced cells were stained for tNGFR and analysed by flow cytometry on a
199 LSR II Fortessa (BD Biosciences).

200 **THP-1 transduction**

201 THP-1 were transduced with lentiviruses at MOI 1 by spinoculation (800g, 45min, 32°C) in presence of protamine sulfate
202 (100ug/ml, Sigma-Aldrich, P402). Transduced cells were sorted based on tNGFR+ expression using MACSelect LNGFR
203 microbeads (Miltenyi Biotec, 130-091-330).

204 **Monocyte transduction**

205 To transduce monocytes, lentivirus was added 2h after plating of monocytes in RPMI + P/S + 5% human AB serum at a
206 MOI of 10 or 15 in presence of protamine sulfate (100ug/ml, Sigma-Aldrich, P4020). After overnight incubation, medium
207 was changed to RH10. Transduction efficiency was assessed between day 6 and day 12 of differentiation and was defined
208 as %tNGFR+ cells. In general, macrophages with transduction rates below 65% were excluded from experiments. In early
209 experiments assessing IL-10 ChCR macrophage polarization, transduction rates down to 55% were accepted.

210 **IFNγ signaling reporter cells**

211 HEK-Blue™ IFN-γ were transduced with lentiviruses by spinoculation in the presence of 8ug/ml polybrene (SantaCruz,
212 sc-134220). To measure secreted embryonic alkaline phosphatase (SEAP), transduced cells were detached mechanically
213 and seeded in 96-well plate. Cells were incubated with cytokines as indicated for 24h. Thereafter, 30ul of the cell
214 supernatant was incubated with 170ul Quanti-Blue solution (Invivogen, rep-qbs) and incubated for 1h at 37°C. OD was
215 measured at 620nm using Spectramax iD3 plate reader (Molecular Devices).

216 **GFP-Luciferase expressing tumor cells**

217 MDA-MB-231 cell line was transduced with lentiviral construct to express Luciferase and EGFP. Cells were sorted for
218 high EGFP expression on a BD FACSAria III (BD Biosciences).

219 **Flow cytometry analysis**

220 To assess transduction rate and polarization marker expression, macrophages were harvested for flow cytometry by
221 incubation with 5mM EDTA in PBS on ice for 45min, followed by gentle pipetting. Detached macrophages were first

222 treated with True-Stain FcX (Biolegend, 422301) and thereafter stained with antibodies (Table 1). Stained samples were
223 acquired on LSR II Fortessa (BD Life Sciences). Untransduced or mock transduced cells were used as gating control for
224 tNGFR and IL-10Rα/IL-10Rβ/TGFβR2, respectively. Data was analyzed using FlowJo v10.10 software (BD Life
225 Sciences). Median fluorescence intensity (MFI) of polarization marker was normalized to the MFI of the corresponding
226 isotype by subtraction. Corresponding isotype controls were used to gate for CD38+ cells.

227 *Table 1: Flow cytometry antibodies*

Epitope	Fluorochrome	Company	Category Number
anti-mouse	BV421	Biolegend	405317
anti-rat	BV421	Biolegend	405414
CD11b m/h	FITC	Biolegend	101206
CD163	BV711	Biolegend	333630
CD206	PE	BioLegend	321105
CD38	BV605	BioLegend	303532
CD86	BV785	Biolegend	305441
HLA-DR	BV510	BioLegend	307646
IgG1 Isotype	BV711	Biolegend	400167
IgG1 Isotype	PE	BD Pharmingen	555749
IgG1 Isotype	BV605	Biolegend	400161
IgG2b Isotype	BV785	Biolegend	400355
IgG2a Isotype	BV510	Biolegend	400267
IL-10Rα	unconjugated	Biolegend	308802
IL-10Rα	PE	Miltenyi Biotec	130-121-341
IL-10Rβ	unconjugated	R&D Systems	MAB874
IL-10Rβ	APC	R&D Systems	FAB874A
NGFR (CD271)	Alexa Fluor 647	BD Biosciences	560326
NGFR (CD271)	BV510	BD Biosciences	563451
NGFR (CD271)	APC	BioLegend	345108
pSTAT1 (Tyr701)	PE	Biolegend	666403
TGFβR2	PE	Biolegend	399703

228

229 **STAT1 phosphoflow**

230 THP-1 or human primary macrophages were used for STAT1 phosphoflow experiments. THP-1 were plated in round
231 bottom 96-well plates in R10. Macrophages were detached as described for flow cytometry analysis and plated in round
232 bottom ultra low attachment 96-well plates (Corning, 7007) in RH10. Cells were rested for 1h at 37°C and thereafter
233 stimulated for 30min as indicated. Cells were fixed by adding one volume of 4% PFA (Santa Cruz) and 15min incubation
234 at 37°C. Next, cell surface markers were stained before cells were permeabilized with True-Phos Perm Buffer (Biolegend).
235 Cells were stained for intracellular pSTAT1 (Tyr701) and analyzed on LSR II Fortessa (BD Biosciences).

236 **IL10 and TGFB1 expression in TNBC**

237 Gene expression data from 195 TNBC patients were obtained from The Cancer Genome Atlas (TCGA). TNBC patients in
238 the TCGA dataset were previously identified by Lehmann et al.[35] Raw counts were retrieved, preprocessed and normalized
239 using the R package TCGABiolinks (2.33.0) without filtration.[36] Percentile expression of IL10 and TGFB1 across all genes
240 was calculated by dividing the rank expression with the total analyzed genes.

241 **RNA sequencing and analysis**

242 For bulk RNA sequencing (RNAseq), monocytes were transduced and differentiated into macrophages. Macrophages were
243 stimulated for 48h as indicated. Total RNA was extracted using Quiashredder (Qiagen, 79254) and RNeasy Mini Kit
244 (Qiagen, 74104) with on column DNA digestion (Qiagen, 79254). RNAseq was performed at the Functional Genomics
245 Center Zurich (FGCZ). The NovaSeq X Plus (Illumina, Inc, California, USA) was used for cluster generation and
246 sequencing according to standard protocol. Sequencing was paired end 150 bp. Between 28 and 86 million reads were
247 generated per sample. RNAseq analysis was performed using the SUSHI framework,[37] which encompassed the following
248 steps: Read quality was inspected using FastQC,[38] and sequencing adaptors removed using fastp,[39] alignment of the RNA-
249 Seq reads using the STAR aligner,[40] and with the GENCODE human genome build GRCh38.p13 (Release 42) as the
250 reference[41] ; the counting of gene-level expression values using the featureCounts function of the R package Rsubread.[42]
251 Differential expression analysis was performed using the generalized linear model as implemented by the DESeq2
252 Bioconductor R package.[43] Principle component analysis (PCA) was performed using the prcomp function from stats R
253 package. For gene set enrichment analysis (GSEA), differentially expressed genes were ranked by log2 fold change. Gene
254 Ontology (GO) GSEA tests were performed using the gseGO function respectively of the clusterProfiler Bioconductor R
255 package.[44] Hallmark and custom pathways GSEA was performed using the GSEA function of the Bioconductor R package
256 clusterProfiler (4.13.0)[44] and the hallmark gene sets (MSigDb 2023.2)[45] on R version (4.4.0). To assess the GSEA of genes
257 upregulated or downregulated in macrophages in anti-PDL-1 responders, genes upregulated or downregulated in baseline
258 tumor macrophages of responders[27] were assembled as custom pathways referred to as responder and non-responder,
259 respectively. Unless stated otherwise, all R functions were executed on R version 4.3.2 (R Core Team, 2020) and
260 Bioconductor version 3.17.

261 **CXCL10 ELISA**

262 To analyze CXCL10 secretion, differentiated macrophages were stimulated for 48h as indicated. Thereafter, supernatant
263 was collected and cell debris removed by centrifugation. Supernatants were stored at -80°C. CXCL10 in supernatant was
264 measured using the ELISA MAX™ Deluxe Set Human CXCL10 (IP-10) kit (Biolegend, 439904). OD450nm and OD570
265 as background were measured using Multiskan SkyHigh plate reader (Thermo Scientific™).

266 **3D spheroid assay**

267 Heterotypic spheroids were generated by mixing 1000 MDA-MB-231 and 1500 MRC-5 cells in Akura™ 96 Spheroid
268 Microplates (InSphero, CS-PB15) in R10. Plates were centrifuged at 100g for 5 min to remove air bubbles and incubated
269 at 37°C, 5% CO_2 overnight. To support the aggregation and maturation of the spheroids, the plates were placed on a tilting
270 stand at a 30° angle. The following day, macrophages were detached using 5mM EDTA in PBS and gentle pipetting and
271 added at a 10:1 ratio (macrophages:MDA-MB-231 at seeding) and stimulated as indicated. Medium and stimuli were
272 replaced every 2-3 days. Fluorescent (EGFP) images were captured using the Cytation 3 (BioTek) with a 4x objective.
273 Images were processed and analyzed with the Gen5 (BioTek) software. To determine the cell number, the mean
274 fluorescence intensity of the full image was determined and the background of an empty well subtracted.

275 **Luciferase assay**

276 To assess an endpoint quantification of tumor cells in the spheroids, luciferase activity of the remaining MDA-MB-231
277 was determined. Spheroids were washed twice with PBS to get rid of luciferase in the supernatant and left with 50 ul

residual PBS per well. 50 ul of BrightGloTM substrate (Promega, E2610) was added per well, consequently leading to cell lysis and release of contained luciferase. The lysate was transferred into a 96-well white plate (Pierce™, 15042). After a minimum waiting time of 2 min, luciferase activity was determined using GloMax® Explorer luminometer (Promega, GM3500). The background signal was determined using a medium control and was subtracted from the samples.

WST1 assay

To assess the ability of genetically engineered macrophages to affect TNBC proliferation, macrophages were stimulated for 2d with IFNγ, IL-10 or TGFβ at indicated concentrations. Supernatants were harvested, clarified by centrifugation and stored at -80°C. For WST1 assay, 5'000 BT-549 or 10'000 MDA-MB-231 cells were plated in 96-well plates. The next day, medium was replaced with supernatants from stimulated macrophages or RH10 as untreated control. 72h after addition of supernatants, viability was measured by incubating cells for 1h with cell proliferation reagent WST-1 (Roche, 5015944001). OD440nm and OD650nm as background were measured using Multiskan SkyHigh plate reader (Thermo Scientific™).

Statistical analysis

The statistical analysis of TCGA and previously published single cell RNAseq data was performed in R (4.4.0). The statistical analysis of bulk RNAseq data was performed using the Sushi framework of the FGCZ.[37] The remaining statistical analysis was performed using Graphpad Prism 10.2.0 using statistical tests specified in the figure legends.

295 # RESULTS

296 ### *IL10* and *TGFB1* are expressed in TNBC

297 IL-10 and TGFβ1 have previously been shown to be expressed in TNBC patients.[19-21] To confirm this data, we analyzed
298 publicly available RNAseq data from 195 TNBC patients for *IL10* and *TGFB1* expression. We found that *IL10* and *TGFB1*
299 were expressed among the top 73% (median) and top 90% (median) genes (figure 1). Thus, TCGA gene expression analysis
300 confirms previously published results of IL10 and TGFβ expression in TNBC patients.

301 ### IL-10 and TGFβ ChCR induce STAT1 signaling

302 To convert IL-10 or TGFβ signals into IFNγ signals, we designed two ChCR, which consist of the extracellular domains
303 of IL10 receptor or TGFβ receptor, respectively, fused to the intracellular domains of the IFNγ receptor (figure 2A and B).
304 To control for transduction efficacy, we also incorporated the truncated NGFR (tNGFR) in the lentiviral vector.

305 In a first instance, we verified IFNγ signaling through the IL-10 ChCR in HEK-Blue IFNγ reporter cell line. In the HEK-
306 Blue IFNγ reporter cell line, IFNγ-induced STAT1 signaling leads to expression of secreted embryonic alkaline
307 phosphatase (SEAP), which can be measured in the supernatant using a colorimetric assay. We stably expressed either the
308 full IL-10 ChCR or the individual components, i.e. IL-10RA fused to IFNGR1 and IL-10RB fused to IFNGR2 in the HEK-
309 Blue IFNγ reporter cells. (online supplemental figure S1A). All cell lines were transduced at >90% efficiency (data not
310 shown) and ChCR expression was confirmed by flow cytometry (online supplemental figure S1B). We found that IL-10
311 induced IFNγ signaling in a dose-dependent manner when the full IL-10 ChCR was expressed (online supplemental figure
312 S1C). Surprisingly, IL-10RA-IFNGR1 alone triggered moderate IFNγ signaling, but both chains of the ChCR were
313 necessary to achieve maximum STAT1 signaling. We also verified that the expression of the full TGFβ ChCR in HEK-
314 Blue IFNγ reporter cell line induced STAT1 signaling (data not shown). Next, we proceeded to the characterization of both
315 ChCRs in the monocyte cell line THP-1, which more closely approximates the properties of primary human macrophages.
316 We found a prominent upregulation of IL-10Rα and TGFβR2 and a moderate one of IL10Rβ using flow cytometry (figure
317 2C). We tested several TGFβR1 antibodies, all suffered from non-specificity and therefore we do not have expression data
318 for TGFβR1. Since TGFβR1 is on the first position of the polycistronic vector and TGFβR2 expression is detectable, we
319 assume that TGFβR1 is expressed as well.

320 Importantly, IL-10 and TGFβ induced a dose-dependent activation of STAT1 in IL-10 or TGFβ ChCR expressing THP-1,
321 respectively, (figure 2D). As expected, untransduced and mock transduced THP-1 cells only showed pSTAT1 signaling
322 upon IFNγ stimulation.

323 To investigate the ChCRs in primary macrophages, we first optimized the protocol for transducing monocytes. We achieved
324 a transduction efficiency of 70.2 ± 14.5% (mean±SD) across all vectors (figure 2E). Again, we saw a very prominent
325 upregulation of IL-10Rα and TGFβR2 and a lesser one of IL-10Rβ (figure 2F). IL-10 induced STAT1 activation to a similar
326 level like IFNγ, whereas TGFβ induced only a little, but consistent STAT1 activation in the macrophages expressing the
327 ChCRs (figure 2G). Thus, both IL-10 and TGFβ ChCR variants trigger the IFNγ signaling pathway.

328 ### ChCR expression induces an inflammatory phenotype upon IL-10 / TGFβ stimulation

329 We next assessed whether triggering the ChCRs induces an inflammatory phenotype in primary human macrophages. We
330 focused on the expression of polarization markers typically upregulated on macrophages either upon IFNγ (i.e., HLA-DR,

331 CD38, CD86) or IL-10 stimulation (i.e., CD163). Importantly, both, IL-10 and TGFβ induced the expression of HLA-DR,
332 CD38 and CD86 in the macrophages expressing the corresponding ChCRs (figure 3A and B). Moreover, IL-10 blocked
333 the upregulation of CD163 in IL-10 ChCR transduced macrophages, while IL-10 massively increased its expression in the
334 controls (figure 3A). Notably, CD163 is upregulated in response to IL-10 but not to TGFβ and therefore we did not measure
335 CD163 expression in TGFβ ChCR expressing macrophages. Overall, we found that, ChCR expressing macrophages indeed
336 show a phenotype similar to IFNγ stimulated macrophages upon stimulation with IL10 or TGFβ.

337 **ChCR expressing macrophages have a IFNγ-like transcriptome**

338 Next, we performed RNAseq to extend the characterization of ChCR expressing macrophages. Principle component
339 analysis (PCA) showed that ChCR expressing macrophages stimulated with their corresponding ligand clustered together
340 with IFNγ stimulated-macrophages, indicating a IFNγ-like transcriptome profile induced by stimulation of the ChCRs
341 (figure 4A). As expected, differential gene expression analysis of ChCR expressing macrophages showed the upregulation
342 of many IFNγ stimulated genes upon IL-10 or TGFβ stimulation when compared to mock transduced macrophages
343 stimulated equally (figure 4B). Similarly, gene set enrichment analysis (GSEA) of hallmark gene sets showed that IFNγ
344 stimulated genes, among other *CXCL9/CXCL10/CIITA,* were significantly enriched in ChCR expressing macrophages
345 upon stimulation (figure 4C). Moreover, GSEA of gene ontology biological processes (GO:BP) showed enrichment of
346 genes associated with antigen presentation (MHC-II HLA genes) and several immune related pathways (figure 4D). Thus,
347 we could confirm that ChCR expressing macrophages have an IFNγ-like transcriptome.

348 **ChCR expressing macrophage upregulate genes associated with anti-PD-L1 response in TNBC patients**

349 CXCL9 and CXCL10 have been associated with better response to immunotherapy and a hot TME in TNBC and other
350 tumors.[8 27 28 46] Interestingly, both *CXCL9* and *CXCL10* were upregulated in ChCR expressing macrophages in RNAseq,
351 which we confirmed for CXCL10 by ELISA (figure 5A and B). Zhang et al have performed single cell RNAseq of TNBC
352 patients treated with chemotherapy and anti-PD-L1 and have identified a TAM transcriptome profile associated with anti-
353 PD-L1 response.[27] Thus, we assessed the expression of other genes associated with good response to ICI treatment in our
354 ChCR expressing macrophages upon stimulation. Indeed, 50 (IL-10 ChCR) and 58 (TGFβ ChCR) of 195 response
355 associated genes were also significantly upregulated in ChCR expressing macrophages upon stimulation with the respective
356 ligand in comparison to mock transduced macrophages (data not shown). Moreover, the heatmap analyzing response
357 associated genes shows a cluster of genes also upregulated in ChCR expressing macrophages (figure 5C). Genes also
358 upregulated in ChCR expressing macrophages upon stimulation belong i.e. to hallmark pathways of IFNγ response and
359 allograft rejection (i.e. *CD74, CXCL9, STAT1, SERPING1, B2M…*) and TNFα signaling via NF-κB (i.e. *TNF, NFKBIA,*
360 *CCL4, ICAM1…*). In addition, we have performed gene set enrichment analysis of responder gene set (R, upregulated in
361 anti-PD-L1 responders) and non-responder gene set (NR, downregulated in anti-PD-L1 responders). We found that the
362 responder gene set was indeed enriched in ChCR expressing macrophages upon stimulation with the respective ligand
363 (figure 5D). In contrast, the gene set associated with non-response was not enriched in ChCR expressing macrophages.
364 Thus, the transcriptome of our genetically engineered macrophages could be beneficial for the response to anti-PD-L1
365 therapy.

366 **ChCR expressing macrophages have anti-tumoral activity**

367 Inflammatory macrophages are reported to have anti-tumoral effects.[20 23-25] Therefore, we explored whether ChCR
368 engineered macrophages have an anti-tumoral effect in a heterotypic TNBC spheroid model. This spheroid model consisted

369 of the TNBC cell line MDA-MB-231 and MRC5 fibroblasts. The presence of fibroblasts was essential as MDA-MB-231
370 cells alone did not form spheroids. One day after formation of MDA-MB-231 and MRC-5 spheroids, we added the
371 genetically engineered macrophages. To monitor the viability of MDA-MB-231 cells easily, we engineered the cell line to
372 express both EGFP and luciferase. We used EGFP to measure MDA-MB-231 number by microscopy over time and
373 luciferase activity to determine the end-point cell number. Indeed, the IL-10- or TGFβ ChCR expressing macrophages
374 limited the expansion of MDA-MB-231 spheroid when added together with the corresponding cytokines, as assessed by
375 mean EGFP intensity (figure 6A-D). We observed similar results when measuring the remaining luciferase activity on day
376 6, even though there was only a trend for TGFβ ChCR (figure 6E and F). Next, we were wondering whether the anti-
377 tumoral effect of ChCR expressing macrophages was mediated by soluble factors or cell-contact. We found that supernatant
378 from stimulated ChCR expressing macrophages alone reduced the proliferation of MDA-MB-231 and BT-549 cells (online
379 supplemental figure S2), indicating secreted factors, are, at least in part, responsible for the anti-tumoral effect observed in
380 the spheroid model.

381

382 **DISCUSSION**

383 The cold TME is highly suppressive and makes tumors non-responsive to ICI. The presence of inflammatory macrophages
384 in the TME increases the responsiveness to ICIs [8 27 28] and therefore, TAMs or macrophages recruited to the TME represent
385 a therapeutic target. Here, we developed ChCR expressing macrophages that are designed to switch to inflammatory
386 macrophages in the presence of IL-10 and TGFβ in the TME. We show that ChCR expressing macrophages indeed have a
387 phenotype similar to IFNγ-induced inflammatory macrophages. Importantly, ChCR expressing macrophages also have a
388 direct anti-tumoral activity.

389 In some ways, the TME is a standalone area for the best tumor growth. Immunosuppressive cytokines are prevalent, among
390 other IL-10 and TGFβ. In TCGA RNAseq data, we confirmed that the transcripts of these cytokines are present in TNBC.
391 Therefore, we constructed ChCRs by combining the extracellular domains of the IL-10 and TGFβ receptors with the
392 intracellular signaling domains of the IFNγ receptor to activate macrophages in the TME, leveraging the local enrichment
393 of IL-10 and TGFβ. Please, note that IFNγ is the crucial cytokine for inducing the inflammatory activation of macrophages.
394 To provide flexibility to the ChCRs, we added a glycine-serine linker between the extracellular domains and the
395 transmembrane domains of the ChCRs.[31 32] To ensure targeting the ChCR to the cell surface, we used the signal peptides
396 from the corresponding IFNγR subunit. The characterization in terms of surface expression and signaling clearly showed
397 that we have created functional ChCRs.

398 Our results suggest that ChCR expressing macrophages become inflammatory in response to IL-10 or TGFβ. These ChCR
399 expressing macrophages exhibit several attributes that would allow them to disrupt an immunosuppressive TME. Firstly,
400 RNAseq showed that ChCR expressing macrophages upregulated the expression of the chemokines *CXCL9* and *CXCL10*
401 upon IL-10 or TGFβ stimulation, which we confirmed for CXCL10 by ELISA .Both in TNBC and beyond, there are several
402 studies that underline the importance of CXCL9 and CXCL10 expression in the TME for the efficacy of a checkpoint
403 inhibitor treatment.[8 27 28 46-49] It is noteworthy that Sloas et al. recently reported that macrophages engineered with an IL-
404 10/IFNλ switch receptor, similar to our IL-10 ChCR, led to an increased T cell infiltration into the tumor *in vivo* in a
405 syngeneic tumor mouse model.[50 51] Secondly, HLA-DR and CD86 were also upregulated as determined by flow cytometry.
406 These surface proteins are crucial for T-cell activation and antigen presentation. RNAseq analysis also showed enrichment
407 of pathways associated with antigen presentation. Therefore, we believe that ChCR expressing macrophages could lead to
408 attraction, infiltration and activation of T cells and thereby initiating a positive feedback loop that results in T cells secreting
409 IFNγ, which in turn leads to TAMs adopting an inflammatory phenotype.[29] Ultimately, we show that that ChCR expressing
410 macrophages have a direct anti-tumoral effect when adding to a TNBC spheroid composed of MDA-MB-231 cells and
411 MRC5 fibroblasts. The anti-tumoral effect is, at least partially, mediated by secreted factors, as conditioned medium
412 obtained from ChCR expressing macrophages reduced the viability of the TNBC cells MDA-MB-231 and BT-549. It is
413 well known that macrophages exhibit anti-tumoral activity upon IFNγ and LPS stimulation.[24-26 52] Here we show that IFNγ-
414 like signaling alone via the ChCR render macrophages anti-tumorally active.

415 We noticed that spheroids co-cultured with IL-10 or TGFβ ChCR expressing macrophages showed a reduced spheroid
416 dissemination compared to the controls (data not shown). It is highly speculative but this reduced dissemination may be
417 due to the anti-tumoral activity of the ChCR expressing macrophages, while TAMs commonly promote metastasis [53]

418 We observed differences in the performance of the two ChCR variants evaluated: the TGFβ ChCR responded to a lower
419 dose of TGFβ than the IL-10 ChCR to IL-10 as shown by the STAT1 activation in THP-1 and CXCL10 ELISA in primary

macrophages. These differences could be due to distinct affinities to the corresponding cytokine or distinct activation thresholds of the ChCRs. The difference in activation threshold might be dependent on the combination of extracellular domain with the intracellular domain of the IFNGR2, which is the limiting subunit in inducing signaling.[54] For instance, in the case of the IL-10 ChCR, we fused the low affinity IL-10Rb to IFNGR2 (reviewed in[55]), whereas in the case of TGFβ ChCR, we fused the high affinity TGFβR2 to the IFNGR2.[56] Importantly, in the complex setting of spheroids, macrophages expressing IL-10 ChCR performed similar to macrophages expressing the TGFβ ChCR, when saturating concentrations were used (figure 6). Ultimately, *in vivo* experiments will be needed to assess and compare activity and toxicity of both ChCR variants.

As mentioned above, patients with advanced, PD-L1 positive TNBC benefit from adding pembrolizumab to chemotherapy.[3] TAMs isolated from patients who responded to anti-PD-L1 treatment show a very unique transcriptomic pattern.[27] The RNAseq data we obtained from ChCR expressing macrophages in response to the corresponding cytokines, showed upregulation of key genes associated with better response to PD-L1 ICI. Therefore, we have good reasons to assume that PD1 ICI treatment in concert with adoptively transferred ChCR expressing macrophages could result in an additive or synergistic anti-tumoral activity.

What is the weakness of the data? The ChCR expressing macrophages present several attributes which may render them anti-tumoral active. However, all the assays including the spheroid assays do not recapitulate the complexity of a tumor with its rich cell content, low pH, high levels of adenosine and hypoxia. Spheroid assays at the best try to mimic it. We will push forward and investigate the anti-tumor activity of these ChCR expressing macrophages in vivo in orthotopic TNBCs mouse models.

441 **LITERATURE**

442 1. Foulkes WD, Smith IE, Reis-Filho JS. Triple-negative breast cancer. *N Engl J Med* 2010;363(20):1938-48. doi:
443 10.1056/NEJMra1001389

444 2. Schmid P, Cortes J, Dent R, et al. Overall Survival with Pembrolizumab in Early-Stage Triple-Negative Breast Cancer.
445 *N Engl J Med* 2024 doi: 10.1056/NEJMoa2409932 [published Online First: 20240915]

446 3. Cortes J, Rugo HS, Cescon DW, et al. Pembrolizumab plus Chemotherapy in Advanced Triple-Negative Breast Cancer.
447 *N Engl J Med* 2022;387(3):217-26. doi: 10.1056/NEJMoa2202809

448 4. Cappell KM, Kochenderfer JN. Long-term outcomes following CAR T cell therapy: what we know so far. *Nat Rev Clin*
449 *Oncol* 2023;20(6):359-71. doi: 10.1038/s41571-023-00754-1 [published Online First: 20230413]

450 5. Albelda SM. CAR T cell therapy for patients with solid tumours: key lessons to learn and unlearn. *Nat Rev Clin Oncol*
451 2024;21(1):47-66. doi: 10.1038/s41571-023-00832-4 [published Online First: 20231030]

452 6. Newick K, O'Brien S, Moon E, Albelda SM. CAR T Cell Therapy for Solid Tumors. *Annu Rev Med* 2017;68:139-52.
453 doi: 10.1146/annurev-med-062315-120245 [published Online First: 20161117]

454 7. Geng P, Chi Y, Yuan Y, et al. Novel chimeric antigen receptor T cell-based immunotherapy: a perspective for triple-
455 negative breast cancer. *Front Cell Dev Biol* 2023;11:1158539. doi: 10.3389/fcell.2023.1158539 [published Online
456 First: 20230629]

457 8. Hammerl D, Martens JWM, Timmermans M, et al. Spatial immunophenotypes predict response to anti-PD1 treatment
458 and capture distinct paths of T cell evasion in triple negative breast cancer. *Nat Commun* 2021;12(1):5668. doi:
459 10.1038/s41467-021-25962-0 [published Online First: 2021/09/29]

460 9. Li F, Li C, Cai X, et al. The association between CD8+ tumor-infiltrating lymphocytes and the clinical outcome of cancer
461 immunotherapy: A systematic review and meta-analysis. *EClinicalMedicine* 2021;41:101134. doi:
462 10.1016/j.eclinm.2021.101134 [published Online First: 20210916]

463 10. Gruosso T, Gigoux M, Manem VSK, et al. Spatially distinct tumor immune microenvironments stratify triple-negative
464 breast cancers. *J Clin Invest* 2019;129(4):1785-800. doi: 10.1172/JCI96313 [published Online First: 2019/02/13]

465 11. Galon J, Bruni D. Approaches to treat immune hot, altered and cold tumours with combination immunotherapies. *Nat*
466 *Rev Drug Discov* 2019;18(3):197-218. doi: 10.1038/s41573-018-0007-y

467 12. de Jong VMT, Wang Y, Ter Hoeve ND, et al. Prognostic Value of Stromal Tumor-Infiltrating Lymphocytes in Young,
468 Node-Negative, Triple-Negative Breast Cancer Patients Who Did Not Receive (neo)Adjuvant Systemic Therapy.
469 *J Clin Oncol* 2022;40(21):2361-74. doi: 10.1200/JCO.21.01536 [published Online First: 20220330]

470 13. Park JH, Jonas SF, Bataillon G, et al. Prognostic value of tumor-infiltrating lymphocytes in patients with early-stage
471 triple-negative breast cancers (TNBC) who did not receive adjuvant chemotherapy. *Ann Oncol* 2019;30(12):1941-
472 49. doi: 10.1093/annonc/mdz395

473 14. Nederlof I, Isaeva OI, de Graaf M, et al. Neoadjuvant nivolumab or nivolumab plus ipilimumab in early-stage triple-
474 negative breast cancer: a phase 2 adaptive trial. *Nat Med* 2024 doi: 10.1038/s41591-024-03249-3 [published
475 Online First: 20240916]

476 15. Keren L, Bosse M, Marquez D, et al. A Structured Tumor-Immune Microenvironment in Triple Negative Breast Cancer
477 Revealed by Multiplexed Ion Beam Imaging. *Cell* 2018;174(6):1373-87 e19. doi: 10.1016/j.cell.2018.08.039
478 [published Online First: 2018/09/08]

479 16. Combes AJ, Samad B, Tsui J, et al. Discovering dominant tumor immune archetypes in a pan-cancer census. *Cell*
480 2022;185(1):184-203 e19. doi: 10.1016/j.cell.2021.12.004 [published Online First: 20211227]

481 17. Franklin RA, Liao W, Sarkar A, et al. The cellular and molecular origin of tumor-associated macrophages. *Science*
482 2014;344(6186):921-5. doi: 10.1126/science.1252510 [published Online First: 20140508]

483 18. Mosser DM, Edwards JP. Exploring the full spectrum of macrophage activation. *Nat Rev Immunol* 2008;8(12):958-69.
484 doi: 10.1038/nri2448

485 19. Toney NJ, Opdenaker LM, Cicek K, et al. Tumor-B-cell interactions promote isotype switching to an
486 immunosuppressive IgG4 antibody response through upregulation of IL-10 in triple negative breast cancers. *J*
487 *Transl Med* 2022;20(1):112. doi: 10.1186/s12967-022-03319-5 [published Online First: 20220307]

488 20. Chen Z, Wu J, Wang L, et al. Tumor-associated macrophages of the M1/M2 phenotype are involved in the regulation
489 of malignant biological behavior of breast cancer cells through the EMT pathway. *Med Oncol* 2022;39(5):83. doi:
490 10.1007/s12032-022-01670-7 [published Online First: 20220516]

491 21. Ding MJ, Su KE, Cui GZ, et al. Association between transforming growth factor-beta1 expression and the clinical
492 features of triple negative breast cancer. *Oncol Lett* 2016;11(6):4040-44. doi: 10.3892/ol.2016.4497 [published
493 Online First: 20160426]

494 22. Qian BZ, Pollard JW. Macrophage diversity enhances tumor progression and metastasis. *Cell* 2010;141(1):39-51. doi:
495 10.1016/j.cell.2010.03.014

496 23. Engstrom A, Erlandsson A, Delbro D, Wijkander J. Conditioned media from macrophages of M1, but not M2
497 phenotype, inhibit the proliferation of the colon cancer cell lines HT-29 and CACO-2. *Int J Oncol* 2014;44(2):385-
498 92. doi: 10.3892/ijo.2013.2203 [published Online First: 2013/12/04]

499 24. Pahl JH, Kwappenberg KM, Varypataki EM, et al. Macrophages inhibit human osteosarcoma cell growth after
500 activation with the bacterial cell wall derivative liposomal muramyl tripeptide in combination with interferon-γ.
501 *Journal of Experimental & Clinical Cancer Research* 2014;33

502 25. Georgouli M, Herraiz C, Crosas-Molist E, et al. Regional Activation of Myosin II in Cancer Cells Drives Tumor
503 Progression via a Secretory Cross-Talk with the Immune Microenvironment. *Cell* 2019;176(4):757-74 e23. doi:
504 10.1016/j.cell.2018.12.038 [published Online First: 20190131]

505 26. Yuan A, Hsiao YJ, Chen HY, et al. Opposite Effects of M1 and M2 Macrophage Subtypes on Lung Cancer Progression.
506 *Sci Rep* 2015;5:14273. doi: 10.1038/srep14273 [published Online First: 20150924]

507 27. Zhang Y, Chen H, Mo H, et al. Single-cell analyses reveal key immune cell subsets associated with response to PD-L1
508 blockade in triple-negative breast cancer. *Cancer Cell* 2021;39(12):1578-93 e8. doi: 10.1016/j.ccell.2021.09.010
509 [published Online First: 20211014]

510 28. Schlenker R, Schwalie PC, Dettling S, et al. Myeloid-T cell interplay and cell state transitions associated with
511 checkpoint inhibitor response in melanoma. *Med* 2024 doi: 10.1016/j.medj.2024.03.015 [published Online First:
512 20240404]

513 29. van Elsas MJ, Middelburg J, Labrie C, et al. Immunotherapy-activated T cells recruit and skewlate-stage activated M1-
514 like macrophagesthat are critical for therapeutic efficacy. *Cancer Cell* 2024 doi: 10.1016/j.ccell.2024.04.011
515 [published Online First: 20240509]

516 30. Rannikko JH, Hollmen M. Clinical landscape of macrophage-reprogramming cancer immunotherapies. *Br J Cancer*
517 2024 doi: 10.1038/s41416-024-02715-6 [published Online First: 20240603]

518 31. Chen X, Zaro JL, Shen WC. Fusion protein linkers: property, design and functionality. *Adv Drug Deliv Rev*
519 2013;65(10):1357-69. doi: 10.1016/j.addr.2012.09.039 [published Online First: 20120929]

520 32. van Rosmalen M, Krom M, Merkx M. Tuning the Flexibility of Glycine-Serine Linkers To Allow Rational Design of
521 Multidomain Proteins. *Biochemistry* 2017;56(50):6565-74. doi: 10.1021/acs.biochem.7b00902 [published Online
522 First: 20171207]

523 33. Hallgren J, Tsirigos K, Pedersen MD, et al. DeepTMHMM predicts alpha and beta transmembrane proteins using deep
524 neural networks: bioRxiv, 2022.

525 34. Pertel T, Reinhard C, Luban J. Vpx rescues HIV-1 transduction of dendritic cells from the antiviral state established
526 by type 1 interferon. *Retrovirology* 2011;8(49) doi: https://doi.org/10.1186/1742-4690-8-49

527 35. Lehmann BD, Colaprico A, Silva TC, et al. Multi-omics analysis identifies therapeutic vulnerabilities in triple-negative
528 breast cancer subtypes. *Nat Commun* 2021;12(1):6276. doi: 10.1038/s41467-021-26502-6 [published Online
529 First: 20211101]

530 36. Mounir M, Lucchetta M, Silva TC, et al. New functionalities in the TCGAbiolinks package for the study and integration
531 of cancer data from GDC and GTEx. *PLoS Comput Biol* 2019;15(3):e1006701. doi: 10.1371/journal.pcbi.1006701
532 [published Online First: 20190305]

533 37. Hatakeyama M, Opitz L, Russo G, et al. SUSHI: an exquisite recipe for fully documented, reproducible and reusable
534 NGS data analysis. *BMC Bioinformatics* 2016;17(1):228. doi: 10.1186/s12859-016-1104-8 [published Online
535 First: 20160602]

536 38. Andrews S. FastQC: A Quality Control Tool for High Throughput Sequence Data 2010 [Available from:
537 http://www.bioinformatics.babraham.ac.uk/projects/fastqc/.

538 39. Chen S, Zhou Y, Chen Y, Gu J. fastp: an ultra-fast all-in-one FASTQ preprocessor. *Bioinformatics* 2018;34(17):i884-
539 i90. doi: 10.1093/bioinformatics/bty560

540 40. Dobin A, Davis CA, Schlesinger F, et al. STAR: ultrafast universal RNA-seq aligner. *Bioinformatics* 2013;29(1):15-
541 21. doi: 10.1093/bioinformatics/bts635 [published Online First: 20121025]

542 41. Frankish A, Diekhans M, Jungreis I, et al. Gencode 2021. *Nucleic Acids Res* 2021;49(D1):D916-D23. doi:
543 10.1093/nar/gkaa1087

544 42. Liao Y, Smyth GK, Shi W. The Subread aligner: fast, accurate and scalable read mapping by seed-and-vote. *Nucleic*
545 *Acids Res* 2013;41(10):e108. doi: 10.1093/nar/gkt214 [published Online First: 20130404]

546 43. Love MI, Huber W, Anders S. Moderated estimation of fold change and dispersion for RNA-seq data with DESeq2.
547 *Genome Biol* 2014;15(12):550. doi: 10.1186/s13059-014-0550-8

548 44. Yu G, Wang LG, Han Y, He QY. clusterProfiler: an R package for comparing biological themes among gene clusters.
549 *OMICS* 2012;16(5):284-7. doi: 10.1089/omi.2011.0118 [published Online First: 20120328]

550 45. Liberzon A, Birger C, Thorvaldsdottir H, et al. The Molecular Signatures Database (MSigDB) hallmark gene set
551 collection. *Cell Syst* 2015;1(6):417-25. doi: 10.1016/j.cels.2015.12.004

552 46. House IG, Savas P, Lai J, et al. Macrophage-Derived CXCL9 and CXCL10 Are Required for Antitumor Immune
553 Responses Following Immune Checkpoint Blockade. *Clin Cancer Res* 2020;26(2):487-504. doi: 10.1158/1078-
554 0432.CCR-19-1868 [published Online First: 20191021]

555 47. Qu Y, Wen J, Thomas G, et al. Baseline Frequency of Inflammatory Cxcl9-Expressing Tumor-Associated Macrophages
556 Predicts Response to Avelumab Treatment. *Cell Rep* 2020;32(1):107873. doi: 10.1016/j.celrep.2020.107873

557 48. Litchfield K, Reading JL, Puttick C, et al. Meta-analysis of tumor- and T cell-intrinsic mechanisms of sensitization to
558 checkpoint inhibition. *Cell* 2021;184(3):596-614 e14. doi: 10.1016/j.cell.2021.01.002 [published Online First:
559 20210127]

560 49. Bill R, Wirapati P, Messemaker M, et al. CXCL9:SPP1 macrophage polarity identifies a network of cellular programs
561 that control human cancers. *Science* 2023;381(6657):515-24. doi: 10.1126/science.ade2292 [published Online
562 First: 20230803]

563 50. Sloas C, Beghi S, Huangfu Y, et al. Abstract 5249: Macrophages expressing synthetic cytokine receptors reverse IL10-
564 mediated immunosuppression within solid tumors and promote adaptive immunity. *Cancer Research*
565 2024;84(6_Supplement):5249-49. doi: 10.1158/1538-7445.Am2024-5249

566 51. Sloas C, Beghi S, Huangfu Y, et al. Macrophages expressing synthetic cytokine receptors reverse IL-10 mdiated
567 Immunosuppression within solid tumors and promote adaptive immunity
568 https://74dfcf.p3cdn1.secureserver.net/wp-content/uploads/2024/04/AACR_2024_EM-C_FINAL.pdf2024
569 [accessed 01.10.2024.

570 52. Muller E, Christopoulos PF, Halder S, et al. Toll-Like Receptor Ligands and Interferon-gamma Synergize for Induction
571 of Antitumor M1 Macrophages. *Front Immunol* 2017;8:1383. doi: 10.3389/fimmu.2017.01383 [published Online
572 First: 20171026]

573 53. Lin Y, Xu J, Lan H. Tumor-associated macrophages in tumor metastasis: biological roles and clinical therapeutic
574 applications. *J Hematol Oncol* 2019;12(1):76. doi: 10.1186/s13045-019-0760-3 [published Online First:
575 20190712]

576 54. Bernabei P, Coccia EM, Rigamonti L, et al. Interferon-γ receptor 2 expression as the deciding factor in human T, B,
577 and myeloid cell proliferation or death. *Journal of Leukocyte Biology* 2001;70(6):950-60. doi:
578 10.1189/jlb.70.6.950

579 55. Walter MR. The molecular basis of IL-10 function: from receptor structure to the onset of signaling. *Curr Top Microbiol*
580 *Immunol* 2014;380:191-212. doi: 10.1007/978-3-662-43492-5_9

581 56. Wrana JL, Attisano L, Carcamo J, et al. TGF beta signals through a heteromeric protein kinase receptor complex. *Cell*
582 1992;71(6):1003-14. doi: 10.1016/0092-8674(92)90395-s

583

584 # FIGURE LEGENDS

585 **Figure 1 *IL10* and *TGFB1* are expressed in TNBC patients.** Shown is the percentile expression of *IL10* and *TGFB1*
586 expression across all transcripts in TNBC samples from TCGA database. Each dot represents one patient. n=195 TNBC
587 patients.

588 **Figure 2 IL-10 / TGFβ stimulation induces STAT1 signaling in chimeric cytokine receptors (ChCR) expressing**
589 **THP-1 and primary macrophages** A) Scheme of lentiviral constructs that were used. B) Scheme of ChCR. Binding of
590 IL-10 or TGFβ to the respective ChCR should induce pSTAT1 signaling. Created in BioRender. Traxel, S. (2024)
591 BioRender.com/y85b161 C/D) THP-1 were either left untransduced or transduced with mock, IL-10 ChCR or TGFβ ChCR
592 construct. C) Expression of IL-10Rα, IL-10Rβ and TGFβR2 was assessed by flow cytometry. Shown are representative
593 histograms. Cells are gated on tNGFR+ cells. D) THP-1 were either left untreated, stimulated with 1, 10 or 100ng/ml IL-
594 10 or TGFβ, or 5ng/ml IFNγ for 30min. pSTAT1 signaling was assessed by Phosphoflow. Shown are median fluorescence
595 intensities (MFI's, mean ± SD) in single cells for untransduced or in tNGFR+ cells for mock, IL-10 ChCR or TGFβ ChCR.
596 N=2-3 E/F) Primary human monocytes were either transduced with mock, IL-10 ChCR or TGFβ ChCR construct. E)
597 Transduction efficiency (tNGFR+) was assessed by flow cytometry upon differentiation to macrophages. Shown are %
598 tNGFR+ cells (mean ± SD). N=14-33 F) Expression of IL-10Rα, IL-10Rβ and TGFβR2 was assessed by flow cytometry.
599 Shown are MFIs gated on tNGFR+ cells (mean ± SD) from 4-5 healthy donors from 3-4 independent experiments G)
600 Transduced macrophages were either left untreated or stimulated as indicated for 30min. pSTAT1 signaling was assessed
601 by Phosphoflow. Shown are pSTAT1 MFIs in tNGFR+ cells (mean ± SD) from 4 donors in 4 independent experiments
602 (IL-10 ChCR) or 5 donors in 3 independent experiments (TGFβ ChCR). p-values were calculated by ratio paired t-tests. *
603 $p < 0.05$, ** $p<0.01$, *** $p<0.001$, **** $p<0.00001$

604 **Figure 3 ChCR expressing macrophages have an inflammatory phenotype upon IL-10 or TGFβ stimulation** A/B)
605 Primary human monocytes were either left untransduced or transduced with mock, IL-10 ChCR or TGFβ ChCR construct.
606 After differentiation to macrophages, cells were either left unstimulated or stimulated with 100ng/ml IL-10, 10 or 100ng/ml
607 TGFβ, or 10ng/ml IFNγ. Expression of surface marker was assessed by flow cytometry. A) Shown are median fluorescence
608 intensities (MFIs, mean ± SD) after subtracting isotype MFI or % CD38+ or % CD163+ gated on CD11b+ cells from 3-4
609 healthy donors in 4 independent experiments. B) Shown are MFI (mean ± SD) after subtracting isotype MFI or % CD38+
610 gated on CD11b+ (untransduced) or NGFR+ (transduced) cells from 3 healthy donors in 2 independent experiments. For
611 MFIs, p-values were calculated using ratio paired t-tests. For % positive cells, p-values were calculated using paired t-tests.
612 * $p < 0.05$, ** $p<0.01$, *** $p<0.001$, **** $p<0.00001$

613 **Figure 4 ChCR expressing macrophages have a IFNγ-like transcriptome** A-D) Monocytes were either transduced with
614 mock, IL-10 ChCR or TGFβ ChCR lentivirus. After differentiation to macrophages, cells were either left unstimulated or
615 stimulated with 100ng/ml IL10, 100ng/ml TGFβ or 10ng/ml IFNγ for 2 days. mRNA was isolated and subjected to bulk
616 RNA sequencing. A) Gene expression principal component analysis, n=3 donors B) Differential gene expression analysis
617 of mock transduced versus IL-10 ChCR transduced macrophages upon IL-10 stimulation and mock transduced versus
618 TGFβ ChCR transduced macrophages upon TGFβ stimulation. Genes highlighted in orange are part of hallmark IFNγ
619 pathway. Threshold for Log2 fold changes was set to <-1 or > 1. P-values were calculated using the Wald test and adjusted
620 for multiple comparison using the Benjamini-Hochberg method. Threshold of false discovery rate (FDR) was set to 0.05.
621 n=3 donors. C) Gene set enrichment analysis (GSEA) of hallmark gene sets. Shown is the normalized enrichment score

622 (NES) of the top 5 enriched hallmark gene sets. D) GSEA of Gene ontology (GO) / biological processes (BP) gene set.
623 Shown is the NES of top 10 enriched BP.

624 **Figure 5 ChCR expressing macrophages upregulate genes associated with good response to anti-PDL-1 treatment**
625 A-D) Monocytes were either transduced with mock, IL-10 ChCR or TGFβ ChCR lentivirus. After differentiation to
626 macrophages, cells were either left unstimulated or stimulated with 100ng/ml IL10, 100ng/ml TGFβ or 10ng/ml IFNγ for
627 2 days. A) mRNA was isolated and subjected to bulk RNA sequencing. *CXCL9* and *CXCL10* expression analyzed by bulk
628 RNAseq. Shown are normalized log2 counts (mean ± SD). N=3 donors. P-values were calculated using the Wald test and
629 adjusted for multiple comparison using the Benjamini-Hochberg method. * False discovery rate (FDR) < 0.05, **
630 FDR<0.01, *** FDR<0.001, **** FDR<0.00001 B) Supernatants were collected and analyzed by CXCL10 ELISA. Shown
631 are CXCL10 concentration (mean ± SD). N=4 donors analyzed in 2-3 independent experiments. p-values were calculated
632 using paired t-tests. * p < 0.05, ** p<0.01, *** p<0.001, **** p<0.00001 C-D) mRNA was isolated and subjected to bulk
633 RNA sequencing. C) Heatmap of genes enriched in response associated with response to anti-PD-L1 treatment in TNBC
634 patients.[27] Expression in genetically engineered macrophages is shown. D) Gene set enrichment analysis of genes expressed
635 in macrophages and associated with response (R) and no response (NR) to anti-PD-L1 treatment in TNBC patients.[27]

636 **Figure 6 ChCR expressing macrophages have anti-tumoral activity** A-F) Monocytes were either left untransduced or
637 transduced with mock, IL-10 or TGFβ ChCR and were differentiated to macrophages. Spheroids were formed by mixing
638 1000 MDA-MB-231 TNBC cells and 1500 MRC-5 fibroblasts. 1 day later, genetically engineered macrophages were added
639 at a 1:10 ratio (MDA-MB-231: macrophages). Spheroids were either left unstimulated, stimulated with IL-10 (100ng/ml),
640 TGFβ (10ng/ml), or IFNγ (10ng/ml). A/B) Quantification of tumor cells in spheroids by measuring mean EGFP intensity
641 (mean ± SD) over time. Shown are results from 3 donors from 2 independent experiments. C/D) Quantification of tumor
642 cells in spheroids by measuring mean EGFP intensity (mean ± SD) 6d after adding macrophages. Shown are results from
643 3 donors from 2 independent experiments. E/F) Quantification of tumor cells in spheroid by measuring luciferase activity
644 6d after adding macrophages. Shown are relative light units (RLU) (mean ± SD) after subtraction of background RLU from
645 3 donors analyzed in 2 independent experiments. p-values were calculated using paired t-tests comparing the ChCRs with
646 mock condition. * p < 0.05, ** p<0.01, *** p<0.001, **** p<0.00001

FIGURES

Figure 1

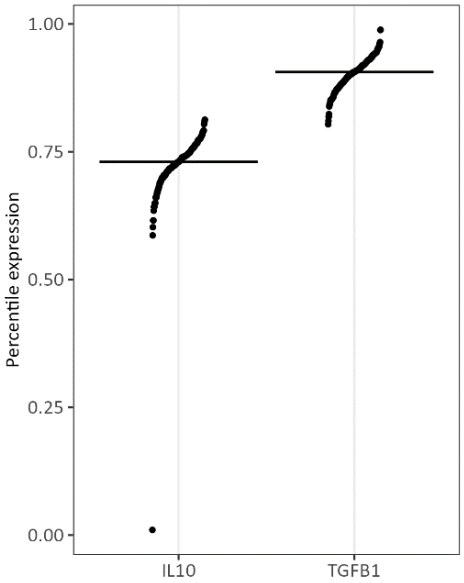

Figure 2

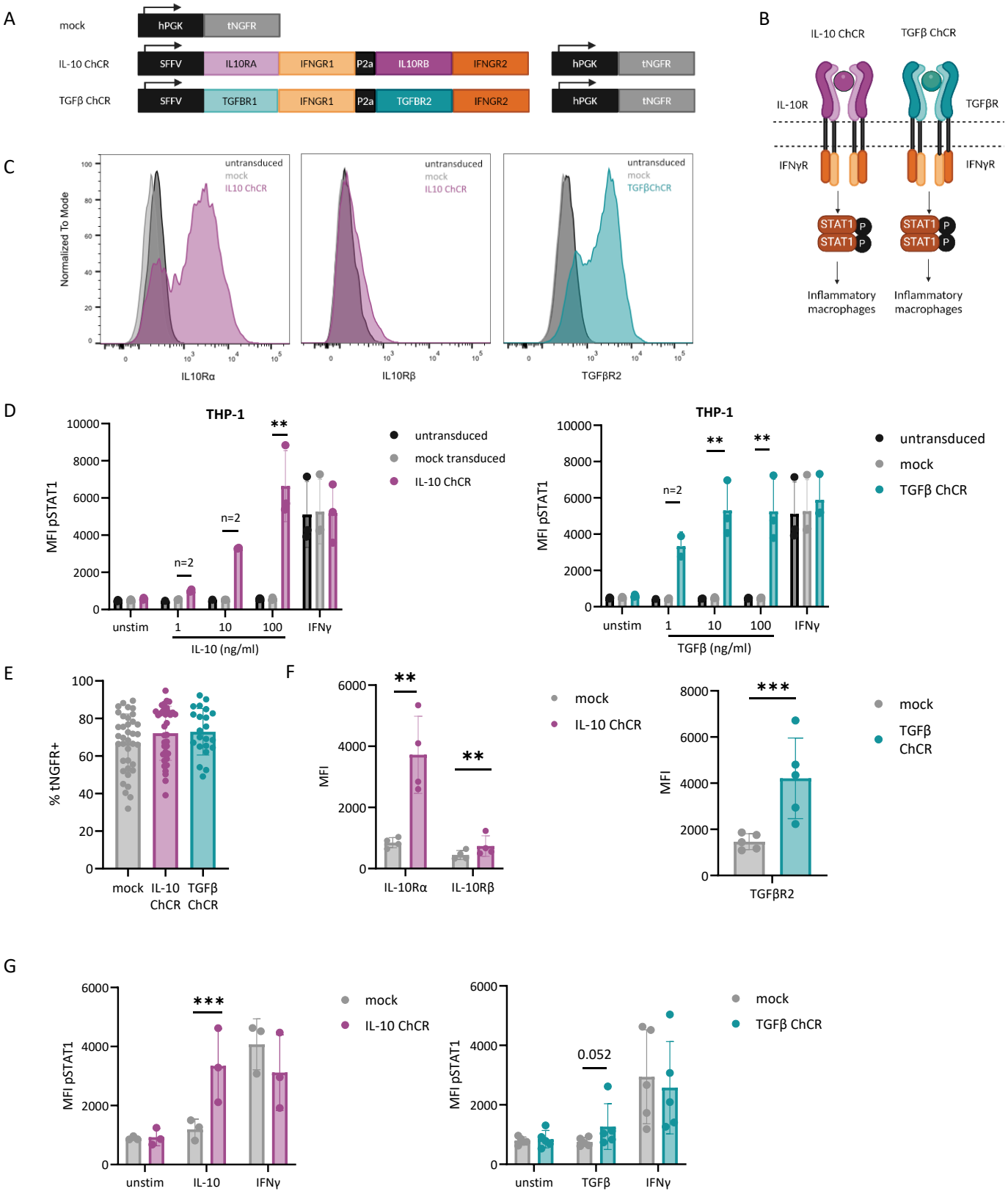
A
mock
hPGK
tNGFR
IL-10 ChCR
SFV
IL10RA
IFNGR1
P2a
IL10RB
IFNGR2
TGFβ ChCR
TGFBR1
TGFBR2
B
IL-10 ChCR
TGFβ ChCR
IL-10R
TGFβR
IFNγR
STAT1
P
Inflammatory macrophages
C
Normalized To Mode
untransduced
mock
IL10 ChCR
TGFβChCR
IL10Rα
IL10Rβ
TGFβR2
D
THP-1
MFI pSTAT1
untransduced
mock transduced
IL-10 ChCR
mock
TGFβ ChCR
n=2
unstim
IFNγ
IL-10 (ng/ml)
TGFβ (ng/ml)
E
% tNGFR+
mock
IL-10 ChCR
TGFβ ChCR
F
MFI
IL-10Rα
IL-10Rβ
TGFβR2
G
MFI pSTAT1
unstim
IL-10
IFNγ
TGFβ
0.052

Figure 3

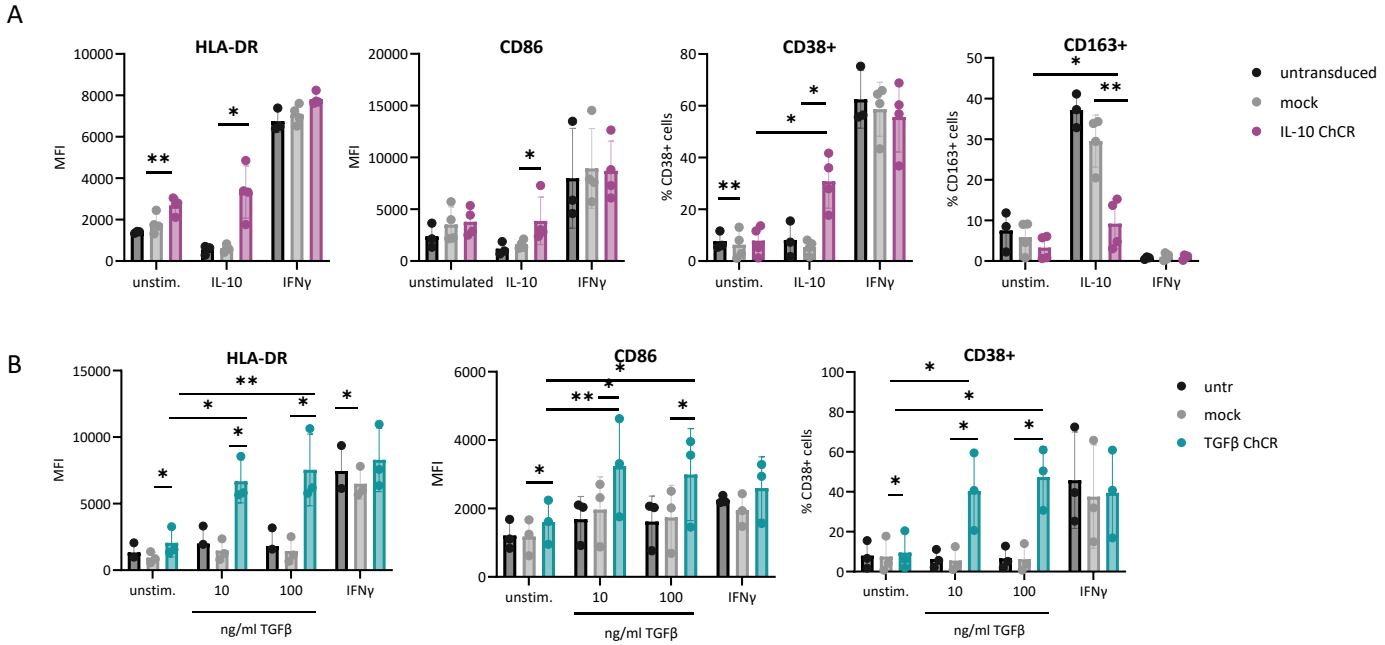
A
HLA-DR
MFI
10000
8000
6000
4000
2000
0
unstim.
IL-10
IFNγ
CD86
MFI
20000
15000
10000
5000
0
unstimulated
IL-10
IFNγ
CD38+
% CD38+ cells
80
60
40
20
0
unstim.
IL-10
IFNγ
CD163+
% CD163+ cells
50
40
30
20
10
0
unstim.
IL-10
IFNγ
untransduced
mock
IL-10 ChCR
B
HLA-DR
MFI
15000
10000
5000
0
unstim.
10
100
IFNγ
ng/ml TGFβ
CD86
MFI
6000
4000
2000
0
unstim.
10
100
IFNγ
ng/ml TGFβ
CD38+
% CD38+ cells
100
80
60
40
20
0
unstim.
10
100
IFNγ
ng/ml TGFβ
untr
mock
TGFβ ChCR

Figure 4

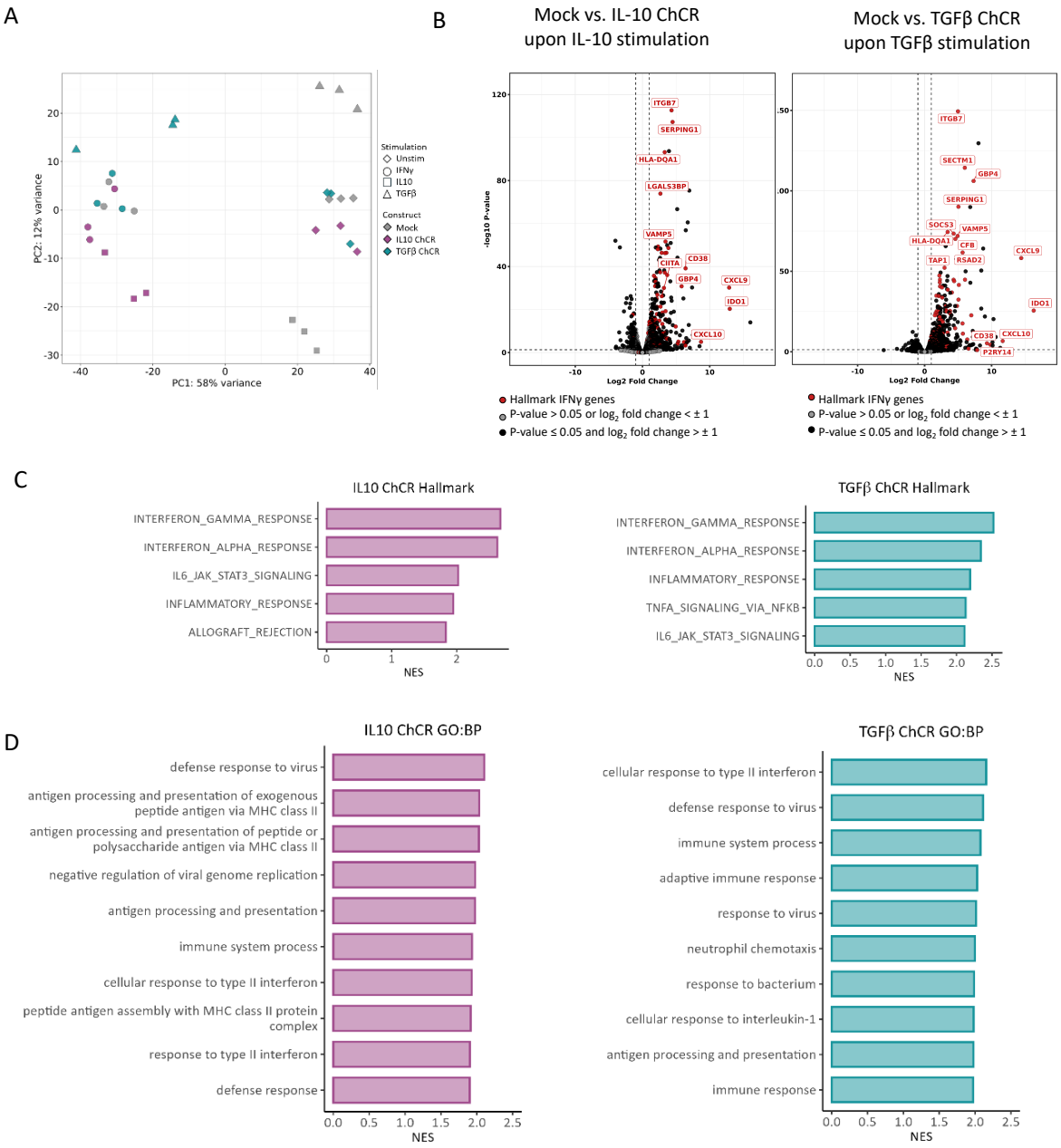
A
PC2: 12% variance
PC1: 58% variance
Stimulation
Unstim
IFNγ
IL10
TGFβ
Construct
Mock
IL10 ChCR
TGFβ ChCR
B
Mock vs. IL-10 ChCR
upon IL-10 stimulation
Mock vs. TGFβ ChCR
upon TGFβ stimulation
-log10 P-value
Log2 Fold Change
ITGB7
SERPING1
HLA-DQA1
LGALS3BP
VAMP5
CIITA
CD38
GBP4
CXCL9
IDO1
CXCL10
SECTM1
SOCS3
CFB
TAP1
RSAD2
P2RY14
Hallmark IFNγ genes
P-value > 0.05 or log2 fold change < ± 1
P-value ≤ 0.05 and log2 fold change > ± 1
C
IL10 ChCR Hallmark
INTERFERON_GAMMA_RESPONSE
INTERFERON_ALPHA_RESPONSE
IL6_JAK_STAT3_SIGNALING
INFLAMMATORY_RESPONSE
ALLOGRAFT_REJECTION
NES
TGFβ ChCR Hallmark
INTERFERON_GAMMA_RESPONSE
INTERFERON_ALPHA_RESPONSE
INFLAMMATORY_RESPONSE
TNFA_SIGNALING_VIA_NFKB
IL6_JAK_STAT3_SIGNALING
NES
D
IL10 ChCR GO:BP
defense response to virus
antigen processing and presentation of exogenous peptide antigen via MHC class II
antigen processing and presentation of peptide or polysaccharide antigen via MHC class II
negative regulation of viral genome replication
antigen processing and presentation
immune system process
cellular response to type II interferon
peptide antigen assembly with MHC class II protein complex
response to type II interferon
defense response
NES
TGFβ ChCR GO:BP
cellular response to type II interferon
defense response to virus
immune system process
adaptive immune response
response to virus
neutrophil chemotaxis
response to bacterium
cellular response to interleukin-1
antigen processing and presentation
immune response
NES

Figure 5

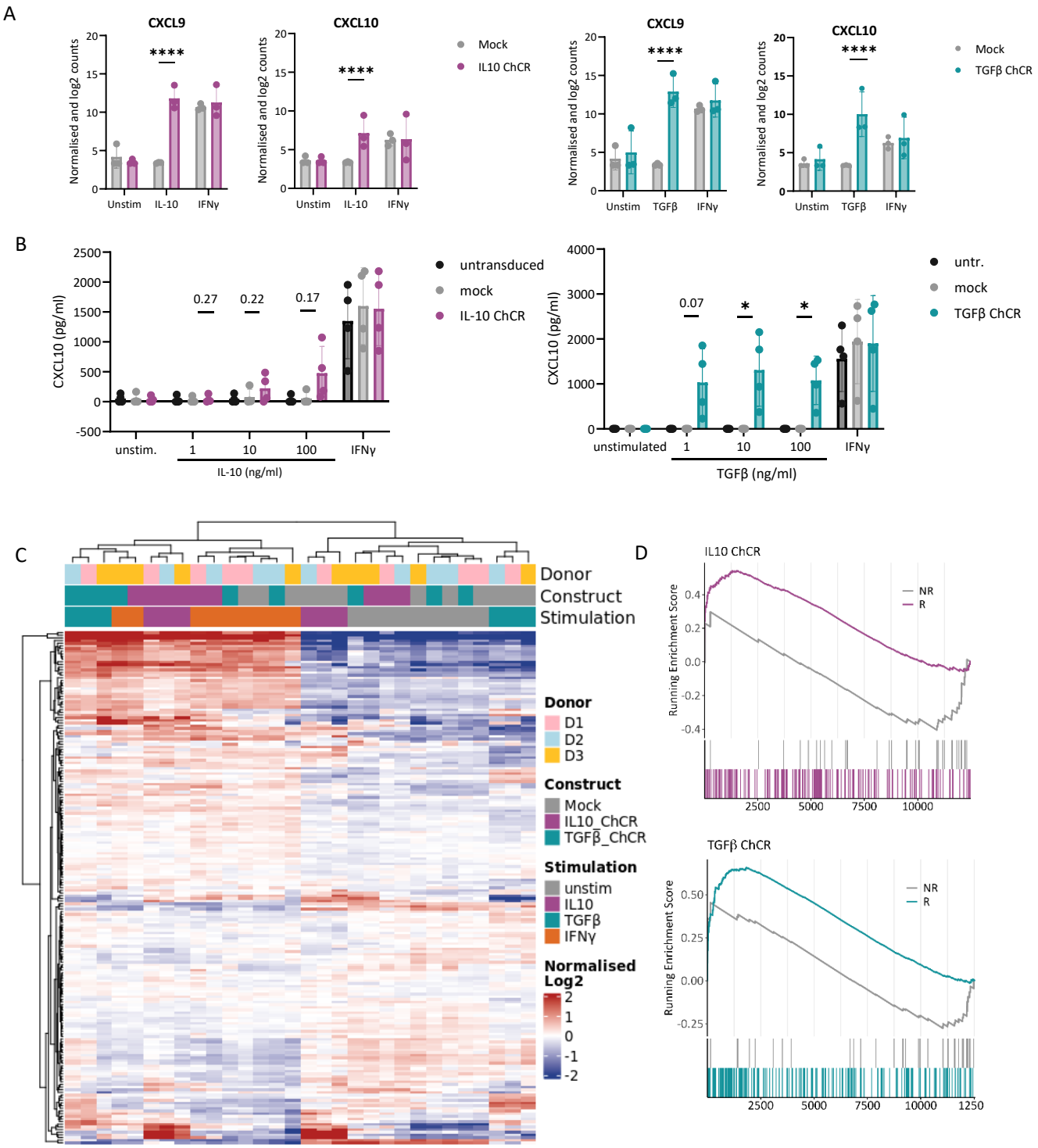
A
CXCL9
CXCL10
Normalised and log2 counts
****
Unstim
IL-10
IFNγ
Mock
IL10 ChCR
TGFβ
TGFβ ChCR
B
CXCL10 (pg/ml)
0.27
0.22
0.17
unstim.
1
10
100
IFNγ
IL-10 (ng/ml)
untransduced
mock
IL-10 ChCR
0.07
*
unstimulated
TGFβ (ng/ml)
untr.
C
Donor
Construct
Stimulation
D1
D2
D3
Mock
IL10_ChCR
TGFβ_ChCR
unstim
IL10
TGFβ
IFNγ
Normalised Log2
D
IL10 ChCR
Running Enrichment Score
NR
R
TGFβ ChCR

Figure 6

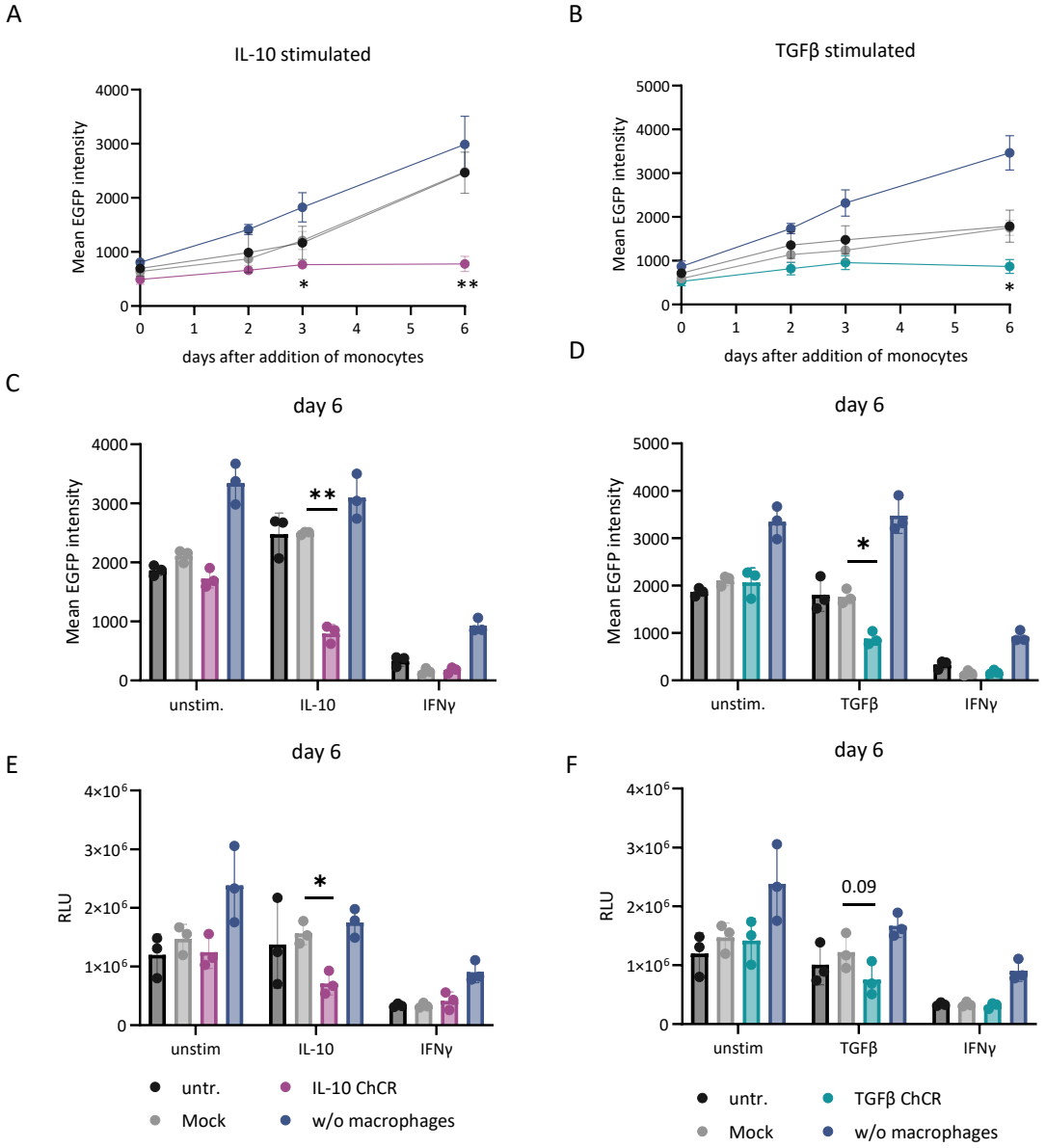
A
IL-10 stimulated
Mean EGFP intensity
4000
3000
2000
1000
0
0 1 2 3 4 5 6
days after addition of monocytes
*
**
B
TGFβ stimulated
Mean EGFP intensity
5000
4000
3000
2000
1000
0
0 1 2 3 4 5 6
days after addition of monocytes
*
C
day 6
Mean EGFP intensity
4000
3000
2000
1000
0
**
unstim.
IL-10
IFNγ
D
day 6
Mean EGFP intensity
5000
4000
3000
2000
1000
0
*
unstim.
TGFβ
IFNγ
E
day 6
RLU
4×10⁶
3×10⁶
2×10⁶
1×10⁶
0
*
unstim
IL-10
IFNγ
untr.
IL-10 ChCR
Mock
w/o macrophages
F
day 6
RLU
4×10⁶
3×10⁶
2×10⁶
1×10⁶
0
0.09
unstim
TGFβ
IFNγ
untr.
TGFβ ChCR
Mock
w/o macrophages

ONLINE SUPPLEMENTAL FIGURES

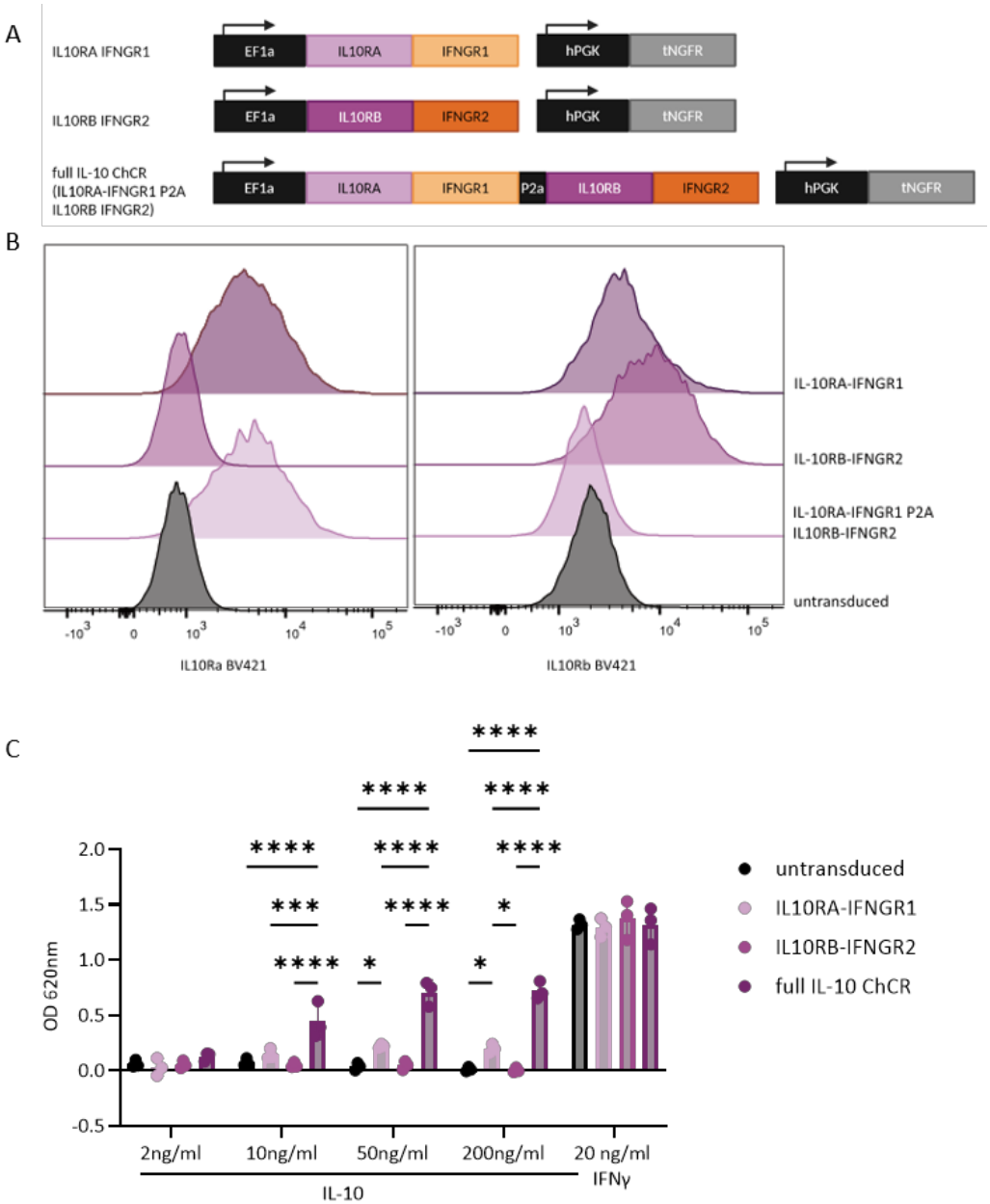

Online supplemental figure S1 IL10 ChCR induces pSTAT1 signaling in HEK-Blue IFNγ reporter cell line. A) Scheme of IL10 ChCR constructs with single chain constructs (IL10RA- IFNGR1and IL10RB-IFNGR2) and the construct containing both chains (IL10RA-IFNGR1 P2A IL10RB-IFNGR2). B) IL10Ra and IL10Rb expression in HEK-Blue transduced with IL10Ra ChCR, IL10Rb ChCR and IL10Rab ChCR. Expression of IL10Ra and IL10Rb was analyzed by flow cytometry. C) HEK-Blue cells were either left untransduced or transduced with IL10Ra ChCR, IL10Rb ChCR or IL10Rab ChCR. Cells were stimulated as indicated for 24h. IFNγ signaling activity was measured using Quanti-Blue assay. Shown is OD 620nm from three independent experiments. P-values were calculated using 2-way ANOVA and multiple comparison with Tukey correction for multiple comparison. * $p < 0.05$, ** $p<0.01$, *** $p<0.001$, **** $p<0.00001$

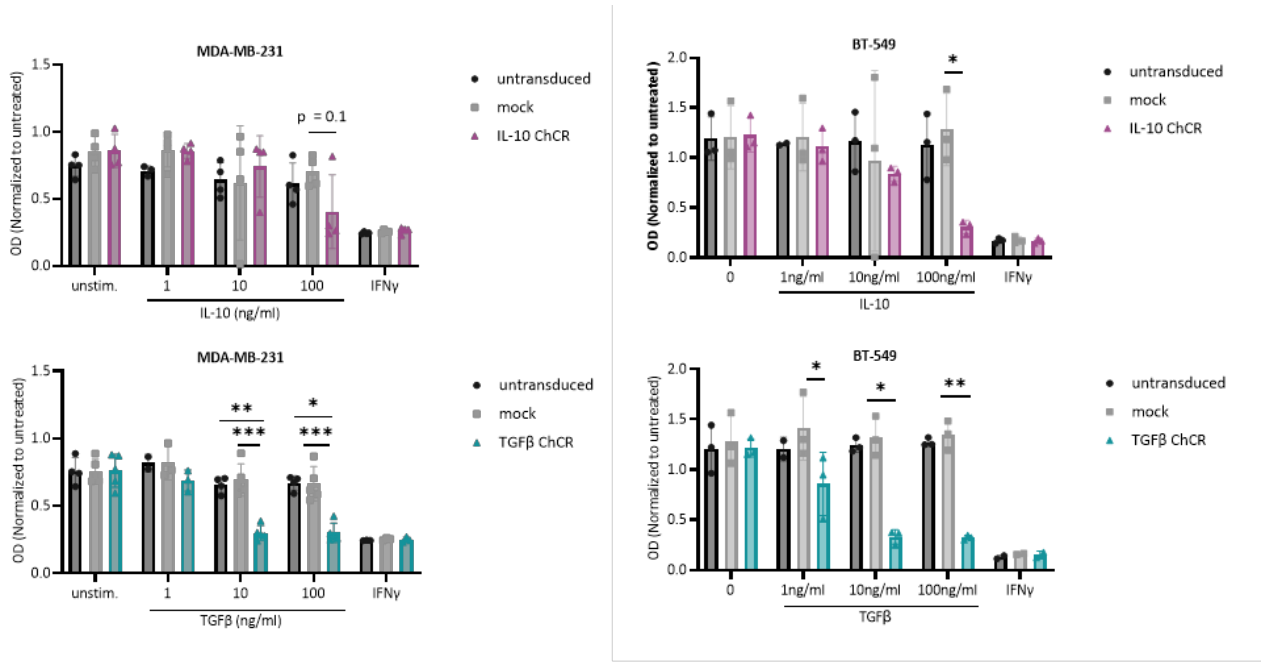

Online supplemental figure S2: Conditioned medium of ChCR expressing macrophages affects viability of MDA-MB-231 and BT-549. Monocytes were transduced, differentiated to macrophages and stimulated for 2 days as indicated. Generated conditioned medium was used to treat MDA-MB-231 or BT-549 cell line for 3 days. Viability was measured by WST-1 assay. Shown are results from using conditioned medium from 3-5 donors. p-values were calculated using paired t-test by comparing ChCR vs. mock for each stimulation. * $p < 0.05$, ** $p<0.01$, *** $p<0.001$, **** $p<0.00001$

SUPPLEMENTARY TABLE

Supplementary Table 1: Uniprot aminoacid (AA) sequences used for the design of the ChCR chains

	Signal peptide	Extracellular domain	Linker	Transmembrane domain	Cytosolic domain
IL10RA ChCR	IFNGR1 AA1-17	IL10RA AA22-235	Glycine serine	IFNGR1 AA246-266	IFNGR1 AA267-489
IL10RB ChCR	IFNGR2 AA1-21	IL10RB AA20-220	Glycine serine	IFNGR2 AA248-268	IFNGR2 AA269-337
TGFBR1 ChCR	IFNGR1 AA1-17	TGFBR1 AA34-126	Glycine serine	IFNGR1 AA246-266	IFNGR1 AA267-489
TGFBR2 ChCR	IFNGR2 AA1-21	TGFBR2 AA23-166	Glycine serine	IFNGR2 AA248-268	IFNGR2 AA269-337